

# Extension of the Trotterized Unitary Coupled Cluster to Triple Excitations

Mohammad Haidar,\* Marko J. Rančić, Yvon Maday, and Jean-Philip Piquemal\*



Cite This: *J. Phys. Chem. A* 2023, 127, 3543–3550



Read Online

ACCESS |



Metrics & More

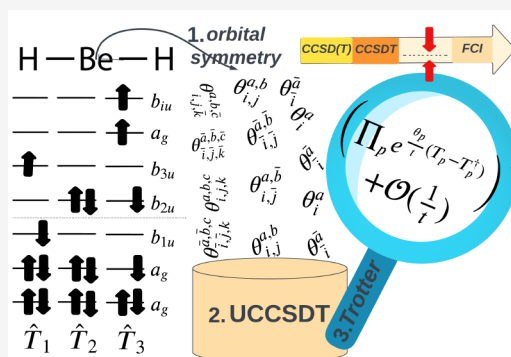


Article Recommendations



Supporting Information

**ABSTRACT:** The Trotterized Unitary Coupled Cluster Single and Double (UCCSD) ansatz has recently attracted interest due to its use in Variation Quantum Eigensolver (VQE) molecular simulations on quantum computers. However, when the size of molecules increases, UCCSD becomes less interesting as it cannot achieve sufficient accuracy. Including higher-order excitations is therefore mandatory to recover the UCC's missing correlation effects. Here, we extend the Trotterized UCC approach via the addition of (true) Triple T excitations introducing UCCSDT. We also include both spin and orbital symmetries. Indeed, in practice, the latter help to reduce unnecessary circuit excitations and thus accelerate the optimization process enabling researchers to tackle larger molecules. Our initial numerical tests (12–14 qubits) show that UCCSDT improves the overall accuracy by at least two orders of magnitude with respect to standard UCCSD. Overall, the UCCSDT ansatz is shown to reach chemical accuracy and to be competitive with the CCSD(T) gold-standard classical method of quantum chemistry.



## INTRODUCTION

The use of quantum computers is a promising strategy to overcome challenges occurring in the area of quantum chemistry.<sup>1–5</sup> Such hardware potentially facilitate the encoding of the full configuration interaction (FCI) wave function of the many-electron molecular system thanks to entangled quantum bits or qubits. In classical computers, the FCI includes a number of determinants which scale exponentially with the number of electrons denoted  $n_e$ , as roughly  $O(n_e^{n_e})$ , where  $n_e$  is the number of spin-orbitals, which makes the manipulation and storage of the wave function inefficient.<sup>6–8</sup> However, using a quantum computer, we can instead store the (FCI) wave function by using only  $n_e$  orbitals which corresponds to  $n_e$  qubits.<sup>1</sup> This potential quantum advantage has recently excited both hardware and software communities generating rapid progress in the field. Several quantum algorithms have been developed, and among them, the Variational Quantum Eigensolver (VQE)<sup>9–12</sup> appears well suited for its practical implementation on present Noisy Intermediate Scaled Quantum (NISQ) devices.<sup>13,14</sup> VQE simulations have been performed numerically for molecules using various virtual noiseless simulators<sup>15–18</sup> and have been tested experimentally on actual NISQ devices.<sup>9,19–22</sup> An important component in VQE is the parametrized ansatz, which represents the trial wave function and is implemented as a quantum circuit, composed of unitary quantum gates, that measures the energy expectation value of the trial wave function and then its parameters are updated in a classical optimization loop. The

Unitary Coupled-Cluster (UCC) ansatz was used when VQE was initially proposed and has gained lots of attention since then. Indeed, UCC includes several attractive features: (i) It is chemistry-inspired since it is a unitary version of the classical coupled-cluster method, which is among the most accurate classical quantum chemistry methods for many-body simulation (see exhaustive recent reviews in refs 23 and 24); (ii) A variant of the UCC theory including single (S) and double (D) excitations called UCCSD is well suited for a direct use on the current NISQ circuits (see comprehensive reviews of UCCSD in refs 25 and 26). Moreover, the Suzuki–Trotter approximation<sup>27</sup> allows separating out the ansatz into a product form of individual exponentials. This version of the ansatz is then denoted Trotterized UCC. Since it is unitary, it can be easily transformed into well-defined unitary gates and therefore its implementation is possible on NISQ devices.

The Trotterized UCCSD ansatz is well documented<sup>25,26,28–30</sup> and has been successfully tested for small molecules.<sup>31–33</sup> However, UCCSD exhibits a limited accuracy in strongly correlated systems similarly as the classical CCSD ansatz.<sup>29,34</sup> Moreover, when the size of the molecules increases,

**Received:** March 15, 2023

**Revised:** March 29, 2023

**Published:** April 11, 2023



many unnecessary excitations can appear in UCCSD which do not improve the chemical accuracy while adding extra noise due to the extra circuit depth.<sup>35</sup> This reveals the need for more accurate and compact representations of the wave function. In that context, various alternative versions of the UCC ansatz, also truncated at the double excitations level, have been proposed by the community and have brought interesting upgrades.<sup>30,36–39</sup> A possible direction also is to use the contracted quantum eigensolvers (CQE) method which provides an ansatz that can generalize CCSD toward FCI.<sup>40,41</sup> However, a possible direction toward improving accuracy is to extend the Trotterized UCCSD through adding three-body clusters that represent the (true) Triple T excitations. For example, the gold-standard CCSD(T) method<sup>42</sup> of (classical) quantum chemistry involves perturbative triple excitations that play a key role in the inclusion of correlation effects.<sup>43</sup>

The objective in this paper is to introduce the Trotterized UCCSDT approach and to analyze the behavior of triple excitations on a set of molecules compared to the initial UCCSD. Of course, an expected downside of the UCCSDT approach is that it involves a large number of parameters to optimize and therefore leads to generation of circuits that are excessively long and therefore not suited for their practical use on current NISQ devices. A possible way to cope with this potential inefficiency of UCCSDT (i.e., allowing to reduce the required number of parameters) is to use the power of the total spin and point group symmetries. Indeed, taking into account these symmetries enables use of spin factorization and orbital symmetry techniques<sup>23</sup> that have been shown to enable simplifications in the classical coupled cluster equations through eliminating unnecessary single and double excitations. Very recently, the point group symmetry constraint has been implemented with the UCCSD ansatz.<sup>18,26</sup> The authors demonstrated a significant reduction of the number of parameters without affecting the accuracy.

This article is organized as follows: the next section is devoted to a description of the theory of Unitary Coupled Cluster method for electronic structure calculations. It includes the detailed formalism of triple excitations. It is given in its simplified form after application of both spin and orbital symmetries. The subsequent section presents the computational materials used to describe the UCCSDT-VQE approach and the last section illustrates the application of UCCSDT-VQE by showing numerical results through testing several molecules. Comparisons were made with UCCSD as well as the classical methods such as CCSD, CCSD(T), CCSDT-full and FCI.

## THEORY

In this work we have based ourselves on the Born–Oppenheimer clamped-nuclei Hamiltonian formalism:

$$\hat{H} = \sum_{p,q} h_{pq} \hat{a}_p^\dagger \hat{a}_q + \frac{1}{2} \sum_{p,q,r,s} h_{pqrs} \hat{a}_p^\dagger \hat{a}_q^\dagger \hat{a}_r \hat{a}_s \quad (1)$$

where  $\hat{a}_p^\dagger$  ( $\hat{a}_q$ ) are anticommuting operators that create (annihilate) electrons in molecular spin–orbital  $p$  ( $q$ ), respectively. The symbols  $h_{pq}$  and  $h_{pqrs}$  denote the one- and two-body integrals of the corresponding operators and spin–orbitals in Dirac notation, respectively. These integrals can be easily computed on a classical computer.

The main goal is to find the ground state energy  $E_0$  of Hamiltonian  $H$  given in eq 1. The Variational Quantum Eigensolver (VQE), a hybrid quantum classical algorithm was designed to solve this problem (see Figure 1 in ref 9). The principal of VQE is that the quantum computer prepares and measures, for any given parameter  $\theta$ , the parametrized quantum state  $|\Psi(\vec{\theta})\rangle$  while the classical computer is used for optimization to propose and update  $\vec{\theta}$ , in order to minimize the variational energy  $\langle \Psi(\vec{\theta}) | H | \Psi(\vec{\theta}) \rangle \geq E_0$ .

We focus on the Unitary Coupled Cluster (UCC) wave function, which, as mentioned in the Introduction, is chemically inspired from the classical Coupled Cluster (CC) method that has yielded high-accuracy results in classical quantum chemistry. The UCC theory is important in our study, since its wave function is unitary and therefore can be efficiently implemented on the quantum computer unlike the regular CC method. The UCC wave function can be expressed as follows:

$$|\Psi(\vec{\theta})\rangle = e^{\hat{T}(\vec{\theta}) - \hat{T}^\dagger(\vec{\theta})} |\psi_{\text{HF}}\rangle \quad (2)$$

where  $\hat{T}$  is the so-called cluster excitation operator and  $\hat{T}^\dagger$  is its Hermitian conjugate.  $|\psi_{\text{HF}}\rangle$  is the reference Hartree–Fock state. Since we are interested in investigating the effect of Triple excitations on UCC's accuracy, the coupled-cluster excitations  $\hat{T}(\vec{\theta})$  are truncated to single, double and triple excitations to introduce UCCSDT,

$$\begin{aligned} \hat{T}(\vec{\theta}) &= \hat{T}_1(\vec{\theta}) + \hat{T}_2(\vec{\theta}) + \hat{T}_3(\vec{\theta}) \\ &= \sum_{a,i} \theta_i^a \hat{a}_a^\dagger \hat{a}_i + \sum_{a,b,i,j} \theta_{ij}^{a,b} \hat{a}_a^\dagger \hat{a}_b^\dagger \hat{a}_i \hat{a}_j \\ &\quad + \sum_{a,b,c,i,j,k} \theta_{ijk}^{a,b,c} \hat{a}_a^\dagger \hat{a}_b^\dagger \hat{a}_c^\dagger \hat{a}_i \hat{a}_j \hat{a}_k \end{aligned} \quad (3)$$

where  $a, b, c \in \text{virt}$ ,  $i, j, k \in \text{occ}$ ,  $\theta_i^a$ ,  $\theta_{ij}^{a,b}$  and  $\theta_{ijk}^{a,b,c}$  are the variational parameters. The triple excitation term  $\hat{T}_3(\vec{\theta})$  (given in eq 3) increases drastically the number of parameters as  $n_o$  increases. This makes the optimization process very difficult and slow to reach convergence. However, as discussed in the Introduction, the many excitations appearing in the UCCSDT wave function (single, double and triple) are not all important and will not affect all the correlation energy. Therefore, determining, *a priori*, those unimportant amplitudes, and thus not including them in eq 3 above before compilation and execution of a variational optimization of the parameters, is highly significant to save resources. In this work we focus only on neutral closed-shell molecular species to make the electronic calculations on such molecules very efficient by exploiting simultaneously both spin and orbital symmetries in the UCCSDT ansatz. Indeed, since in the neutral closed-shell molecules exhibit an even number of electrons, one can maintain only excitations that can satisfy spin symmetry through keeping the balance between spin-up ( $\uparrow$ ) and spin-down ( $\downarrow$ ) electrons. Therefore, it is straightforward to include the spin symmetry constraint in eq 3. The inclusion of orbital symmetry constraints requires more precise explanation for its implementation for each molecule subject to a nontrivial point group symmetry.<sup>44,45</sup> For example, the  $\text{H}_2$  and  $\text{N}_2$  molecules belongs to the  $D_{\infty h}$  point group whereas LiH and  $\text{H}_2\text{O}$  belong to  $C_{\infty v}$ . Each such group is characterized by its irreducible representations (irreps) which are listed in ref 46. Let us now

describe how to impose the orbital symmetry constraint from each irreps group into eq 3 following the rules that are given in chapter 2 of ref 23 and that were recently reviewed in ref 26. First, we use the orbital symmetry operator  $\hat{\xi}_e$ , noted in ref 26, which maps

- each orbital to the irreps of that orbital
- each pair of orbitals to the tensor product of the two irreps of the two orbitals
- each triple of orbitals to the tensor product of the three irreps of the three orbitals

Assuming, e.g., that the  $D_{2h}$  group is used, and taking for example the triple excitation case, if the irreps of  $i, j, k$  are  $i = A_w, j = B_{1g'}$ , and  $k = B_{2w}$  then we have  $\hat{\xi}_e(i) = A_w, \hat{\xi}_e(j) = B_{1g'}$ ,  $\hat{\xi}_e(k) = B_{2w}$  and  $\hat{\xi}_e(i, j, k) = B_{3g}$  according to the multiplication table for  $D_{2h}$ . Then, the complexity reduction comes from the rule that single excitations must only occur between orbitals that belong to the same irreps. Double and Triple excitations must only occur between occupied and virtual orbitals whose tensor product irreps are similar. Furthermore, the products of irreps that are partaken in each excitation must contain the fully symmetric irreps.

Merging these constraints with the spin symmetry, we obtain the operator for Singles (S)

$$\begin{aligned} \hat{T}_1(\vec{\theta}) - \hat{T}_1^\dagger(\vec{\theta}) &= \sum_{\substack{i,a \in \{\uparrow\} \\ \hat{\xi}_e(i) = \hat{\xi}_e(a)}} \theta_i^a (\hat{a}_a^\dagger \hat{a}_i - \hat{a}_i^\dagger \hat{a}_a) + \sum_{\substack{\bar{i}, \bar{a} \in \{\downarrow\} \\ \hat{\xi}_e(\bar{i}) = \hat{\xi}_e(\bar{a})}} \theta_{\bar{i}}^{\bar{a}} (\hat{a}_{\bar{a}}^\dagger \hat{a}_{\bar{i}} - \hat{a}_{\bar{i}}^\dagger \hat{a}_{\bar{a}}) \end{aligned} \quad (4)$$

for Doubles (D),

$$\begin{aligned} \hat{T}_2(\vec{\theta}) - \hat{T}_2^\dagger(\vec{\theta}) &= \sum_{\substack{i < j, a < b \in \{\uparrow\} \\ \hat{\xi}_e(i, j) = \hat{\xi}_e(a, b)}} \theta_{i,j}^{a,b} (\hat{a}_a^\dagger \hat{a}_b^\dagger \hat{a}_j \hat{a}_i - \hat{a}_i^\dagger \hat{a}_j^\dagger \hat{a}_b \hat{a}_a) \\ &+ \sum_{\substack{\bar{i} < \bar{j}, \bar{a} < \bar{b} \in \{\downarrow\} \\ \hat{\xi}_e(\bar{i}, \bar{j}) = \hat{\xi}_e(\bar{a}, \bar{b})}} \theta_{\bar{i}, \bar{j}}^{\bar{a}, \bar{b}} (\hat{a}_{\bar{a}}^\dagger \hat{a}_{\bar{b}}^\dagger \hat{a}_{\bar{j}} \hat{a}_{\bar{i}} - \hat{a}_{\bar{i}}^\dagger \hat{a}_{\bar{j}}^\dagger \hat{a}_{\bar{b}} \hat{a}_{\bar{a}}) \\ &+ \sum_{\substack{i, \bar{j}, a, \bar{b} \\ i, a \in \{\uparrow\}; \bar{j}, \bar{b} \in \{\downarrow\} \\ \hat{\xi}_e(i, \bar{j}) = \hat{\xi}_e(a, \bar{b})}} \theta_{i, \bar{j}}^{a, \bar{b}} (\hat{a}_a^\dagger \hat{a}_{\bar{j}}^\dagger \hat{a}_{\bar{j}} \hat{a}_i - \hat{a}_i^\dagger \hat{a}_{\bar{j}}^\dagger \hat{a}_{\bar{j}} \hat{a}_a) \end{aligned} \quad (5)$$

and for Triples (T),

$$\begin{aligned} \hat{T}_3(\vec{\theta}) - \hat{T}_3^\dagger(\vec{\theta}) &= \sum_{\substack{i < j < k \in \{\uparrow\} \\ a < b < c \in \{\uparrow\} \\ \hat{\xi}_e(i, j, k) = \hat{\xi}_e(a, b, c)}} \theta_{i,j,k}^{a,b,c} (\hat{a}_a^\dagger \hat{a}_b^\dagger \hat{a}_c^\dagger \hat{a}_k \hat{a}_j \hat{a}_i - \hat{a}_i^\dagger \hat{a}_j^\dagger \hat{a}_k^\dagger \hat{a}_c \hat{a}_b \hat{a}_a) \\ &+ \sum_{\substack{\bar{i} < \bar{j} < \bar{k} \in \{\downarrow\} \\ \bar{a} < \bar{b} < \bar{c} \in \{\downarrow\} \\ \hat{\xi}_e(\bar{i}, \bar{j}, \bar{k}) = \hat{\xi}_e(\bar{a}, \bar{b}, \bar{c})}} \theta_{\bar{i}, \bar{j}, \bar{k}}^{\bar{a}, \bar{b}, \bar{c}} (\hat{a}_{\bar{a}}^\dagger \hat{a}_{\bar{b}}^\dagger \hat{a}_{\bar{c}}^\dagger \hat{a}_{\bar{k}} \hat{a}_{\bar{j}} \hat{a}_{\bar{i}} - \hat{a}_{\bar{i}}^\dagger \hat{a}_{\bar{j}}^\dagger \hat{a}_{\bar{k}}^\dagger \hat{a}_{\bar{c}} \hat{a}_{\bar{b}} \hat{a}_{\bar{a}}) \\ &+ \sum_{\substack{i < j, a < b \in \{\uparrow\} \\ \bar{k}, \bar{c} \in \{\downarrow\} \\ \hat{\xi}_e(i, j, \bar{k}) = \hat{\xi}_e(a, b, \bar{c})}} \theta_{i,j,\bar{k}}^{a,b,\bar{c}} (\hat{a}_a^\dagger \hat{a}_b^\dagger \hat{a}_{\bar{c}}^\dagger \hat{a}_{\bar{k}} \hat{a}_j \hat{a}_i - \hat{a}_i^\dagger \hat{a}_j^\dagger \hat{a}_{\bar{k}}^\dagger \hat{a}_{\bar{c}} \hat{a}_b \hat{a}_a) \\ &+ \sum_{\substack{\bar{i} < \bar{j}, \bar{a} < \bar{b} \in \{\downarrow\} \\ k, c \in \{\uparrow\} \\ \hat{\xi}_e(i, \bar{j}, \bar{k}) = \hat{\xi}_e(a, b, \bar{c})}} \theta_{\bar{i}, \bar{j}, \bar{k}}^{a,b,\bar{c}} (\hat{a}_a^\dagger \hat{a}_{\bar{b}}^\dagger \hat{a}_{\bar{k}}^\dagger \hat{a}_c \hat{a}_{\bar{j}} \hat{a}_{\bar{i}} - \hat{a}_{\bar{i}}^\dagger \hat{a}_{\bar{j}}^\dagger \hat{a}_{\bar{k}}^\dagger \hat{a}_c \hat{a}_{\bar{b}} \hat{a}_a) \end{aligned} \quad (6)$$

With these excitations we construct the symmetric UCCSDT, which is named throughout the text as sym-UCCSDT.

## COMPUTATIONAL PROCEDURE

The implementation of an exponential operator  $e^{\hat{T}(\vec{\theta}) - \hat{T}^\dagger(\vec{\theta})}$  given in eq 2 cannot be done directly on quantum hardware. Therefore, applying Trotterization using the Suzuki–Trotter expansion<sup>27</sup> is mandatory to break up the exponential of a sum as a product of individual exponentials. Thus, we used this approach to write the Trotterized  $e^{\hat{T}(\vec{\theta}) - \hat{T}^\dagger(\vec{\theta})}$  with  $\hat{T}(\theta) - \hat{T}^\dagger(\theta)^\dagger$  (eq 3) in the form

$$e^{\hat{T}(\vec{\theta}) - \hat{T}^\dagger(\vec{\theta})} = \left( \prod_{\rho} e^{\theta_{\rho}/t (\hat{T}_{\rho} - \hat{T}_{\rho}^\dagger)} \right)^t + \mathcal{O}\left(\frac{1}{t}\right) \quad (7)$$

where  $t$  is the number of Trotter steps and  $\rho$  corresponds to the elements of excitations introduced in eq 3. The essential tools needed to perform the VQE process (such as Fermionic second quantization of  $\hat{H}$  eq 1, Fermion-qubit transforms using Jordan–Wigner representation,<sup>47</sup> Trotterization, etc.) are implemented in the myQLM-Fermion package.<sup>48,49</sup> We use the UCC family module from our OpenVQE package<sup>49,50</sup> to implement UCCSDT excitations (eqs 4–6). We also used the PySCF package<sup>51</sup> to evaluate the molecular orbital integrals  $h_{pq}$  and  $h_{pqrs}$  which are given in eq 1. Using PySCF package, we determine automatically the irreps of each molecular orbital as well as the direct tensor product of the irrep of the molecular spin-orbitals by using the product table.<sup>46</sup> Finally, we used a gradient-based optimization method (BFGS) from the *scipy.optimize* library<sup>52</sup> for optimizing the variational parameters  $\theta_i^a, \theta_{ij}^{a,b}$  and  $\theta_{ijk}^{a,b,c}$ . The gradient norm used is equal to  $10^{-10}$ .

For the calculation of classical chemistry methods CCSD and CCSD(T), we use the PYSCF package. However, for the full CCSDT, we use the CCT3<sup>53</sup> plugin that is provided in the Psi4 package.<sup>53</sup> Given that the CC(t;3) method is supposed to be practically as accurate as full CCSDT for total electronic energies. The energy convergence threshold used is  $10^{-10}$  Ha.

## NUMERICAL RESULTS AND DISCUSSIONS

We tested our UCCSDT-VQE (eq 3) and sym-UCCSDT-VQE (eqs 4–6) methods on three sets of molecules: LiH, BeH<sub>2</sub> and H<sub>2</sub>O. For sym-UCCSD and sym-UCCSDT-VQE calculations, we chose the highest possible Abelian point groups that belong to each of the systems, i.e., by referring to ref 54 we have the  $C_{2v}$  point group for LiH and H<sub>2</sub>O but the  $D_{2h}$  point group for BeH<sub>2</sub>. The minimal STO-3G basis<sup>55</sup> is used in order to minimize the computational costs. Within the STO-3G basis set, LiH has a Hilbert space spanned by 12 hartree–Fock (HF) orbitals (4 occupied, 8 virtual). BeH<sub>2</sub> has 14 HF orbitals (6 occupied, 8 virtual), H<sub>2</sub>O has 14 HF orbitals (10 occupied, 4 virtual). In the multiqubit register, we assign each qubit to a spin-orbital, thus LiH (BeH<sub>2</sub> and H<sub>2</sub>O) is (are) represented by 12 (14) qubits. We used the Quantum Learning Machine<sup>49</sup> (QLM) simulator that is able to simulate up to 40 qubits (with large memory), and we used the noiseless simulation mode (i.e., such an ideal simulator mimics the behavior of performing the experiment with an infinite number of shots) in order to minimize computational run time and memory demands. First, we tested the two methods on the LiH molecule at two bond lengths:  $R = 1.0$  Å and  $R = 3.0$  Å. As shown in Table 1, we observe that UCCSD and sym-UCCSD

Table 1. UCC-VQE Simulations for LiH at Various Bond Lengths:  $R = 1.0 \text{ \AA}$  and  $R = 3.0 \text{ \AA}$ <sup>a</sup>

Method	$R = 1.0 \text{ \AA}$		$R = 3.0 \text{ \AA}$	
	Ener. (Ha)	Err. (Ha)	Ener. (Ha)	Err. (Ha)
UCCSD	-7.78445508682	$5.19 \times 10^{-6}$	-7.7987523587	$9.08 \times 10^{-5}$
sym-UCCSD	-7.78445509065	$5.18 \times 10^{-6}$	-7.79875240726	$9.07 \times 10^{-5}$
UCCSDT(this work)	-7.78446025863	$2.14 \times 10^{-8}$	-7.79884308319	$7.63 \times 10^{-8}$
sym-UCCSDT	-7.78446025863	$2.13 \times 10^{-8}$	-7.79884308642	$7.30 \times 10^{-8}$
FCI (STO-3G)	-7.78446028003		-7.79884315950	

<sup>a</sup>The obtained UCC-energies are in Hartree (Ha). The error (Err) is the difference between the estimated UCC-energy and the FCI (the reference result is given in the last row).

Table 2. UCC-VQE Simulations for LiH, H<sub>2</sub>O and BeH<sub>2</sub> Calculated at Equilibrium<sup>a</sup>

	Qbits	Sym.	Para Bef. (Af.)	%	$\Delta E_{\text{Sym-UCCSD}}^{18}$	$\Delta E_{\text{Sym-UCCSD}}^*$	$\Delta E_{\text{Sym-UCCSDT}}^*$
LiH	12	$C_{2v}$	188 (58)	30.8	$1.09 \times 10^{-5}$	$1.06 \times 10^{-5}$	$2.16 \times 10^{-8}$
H <sub>2</sub> O	14	$C_{2v}$	340 (104)	30.5	$1.09 \times 10^{-4}$	$1.0 \times 10^{-4}$	$2.11 \times 10^{-6}$
BeH <sub>2</sub>	14	$D_{2h}$	644 (92)	14.2	$3.82 \times 10^{-4}$	$3.81 \times 10^{-4}$	$6.63 \times 10^{-6}$

<sup>a</sup>The geometry data are taken from the CCCBDB-NIST Database.<sup>54</sup> Columns 2 and 3 correspond to the number of qubits and to the point group used in each of the molecules, respectively. The original parameters (and the parameters after reduction) are given in the 4th column and the percent of the operators used (i.e., single, double and triple excitations) after parameter reduction are in column 5. The UCC-VQE energy differences compared with the FCI energy (Ha) are shown from the 6th to 8th columns. Data of  $\Delta E_{\text{Sym-UCCSD}}$  are taken from ref 18. The asterisk (\*) represents this work.

brings similar numerical results. A similar observation can be made for the UCCSDT and sym-UCCSDT results. This demonstrates that the presence of spin and orbital symmetries in sym-UCC-VQE reaches the same result as UCC-VQE but in a more efficient way and without influencing the overall accuracy. For example, Table 2 shows that the number of parameters is reduced from 188 to 58 for the case of LiH, which in practice accelerates the optimization due to the fact that a lower-dimensional optimization problem is tackled. We confirm the convergence of sym-UCCSD and sym-UCCSDT energies at gradient norm equal to  $10^{-10}$  inside BFGS optimizer (see the convergence as a function of optimization steps in Figure S1 of the Supporting Information).

As mentioned in the literature,<sup>25,26,30,49,56</sup> testing the Trotterization effect in the UCC ansatz is important since, as seen in equation 7, using  $t > 1$  might in principle, decrease the Trotterization error. Besides the Trotterization study, a different method called the disentangled UCC ansatz<sup>57</sup> has been introduced, and in ref 58 the ordering of operators in this ansatz has been discussed. In our case we are interested in focusing on the Trotterized ansatz truncated at Triple excitations. To test this in our symmetric operators, we use the sym-UCCSD and sym-UCCSDT methods with different Trotter steps  $t$ . It should be noted that when we increased it beyond 1, the same ansatz (and associated parameters) was chosen first and then we extended it. We observe in Table S2 of the Supporting Information that increasing  $t$ , from  $t = 1$  up to  $t = 15$  steps, does not impact the results. A similar conclusion is observed in the sym-UCCSDT case when we increased  $t$  from  $t = 1$  up to  $t = 3$  steps. We have thus carefully checked that most of the operators that are involved in the symmetric version actually do not commute (see Table S3, Supporting Information) so that—a priori—there should be, at least, a slight difference in the optimized discrete energies with different values of  $t$ , but also there should be a difference on the coefficients in front of the operators (results not shown: the coefficients for  $t$  are those obtained for  $t = 1$  divided by  $t$ ). The reason we found is that—a posteriori, i.e., after computation—we verified that, in both cases, the operators

associated with non-negligible coefficients do commute (i.e., the coefficients in front of noncommuting operators are negligible). We do not see reasons for this but it needs to be further analyzed.

In the remaining part of this Article, we therefore use a UCC ansatz truncated at the Single, Double, and Triple excitations using a single Trotter step.

When applying the point group symmetry method, the number of optimization parameters was reduced between 14.2% (case of BeH<sub>2</sub> having a  $D_{2h}$  point group symmetry) and 30.8% (case of LiH having a  $C_{2v}$  point group symmetry), as shown in Table 2. This consequently will significantly reduce the gate cost of implementing triple excitations on quantum computers. Despite this reduction in parameters in the sym-UCCSDT circuit-ansatz, this circuit depth can be still considered as high compared to current NISQ devices capabilities. This is linked to the fact that we are using the CNOT staircase<sup>4,59</sup> method that maps the exponential of each Fermionic excitation into one- and two-qubit gates. Therefore, the number of CNOT (2-qubit gate) increases with the level of excitations: 12 for single, 48 for double and 320 for Triples. Then the circuit depths are 21, 84, 464, respectively. This can be illustrated for example with the BeH<sub>2</sub> case, as shown in Table 2. It contains 92 parameters, associated with the following excitations: 8 singles, 26 doubles, 52 triples, leading to a total CNOT gates in sym-UCCSDT circuit equal to  $12 \times 8 + 48 \times 26 + 320 \times 52 = 17984$ . Attempts for reducing the CNOT counts in triple excitation operators and higher orders have been recently proposed.<sup>60</sup> However, even with this reduction in CNOT counts, UCCSDT ansatzes are not yet amendable to current NISQ devices. Now let us discuss sym-UCCSD and sym-UCCSDT energy errors, one of the main focus in the Article. It is important to note that we will not consider the ordering of operators in the ansatz since it is believed to bring only small accuracy improvements.<sup>30</sup> However, it will, of course, remain of potential interest to further study its impact. We believe that the inclusion of triple excitations should generate a sufficient improvement of the ansatz quality. The energy error we study is the difference

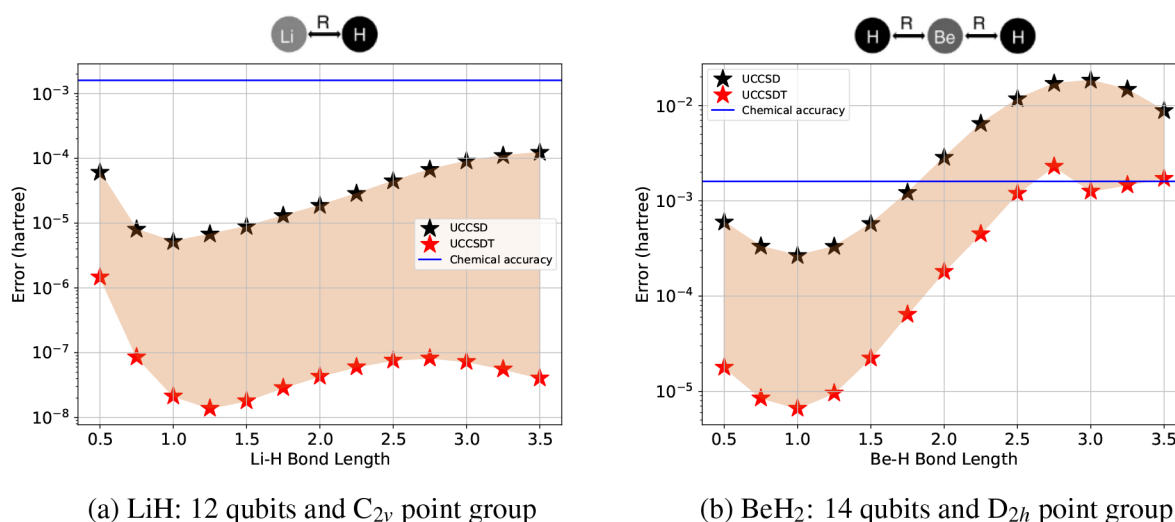


**Figure 1.** Error of the UCCSD and UCCSDT simulations using both spin and point group symmetries for geometries LiH and BeH<sub>2</sub> at different bond lengths. The horizontal blue line represents the chemical accuracy, i.e.,  $1.6 \times 10^{-3}$  Ha.

**Table 3. Error Comparison between Classical Methods (CCSD, CCSD(T) and CCSDT-full) and UCC-VQE (sym-UCCSD and sym-UCCSDT) Simulations for LiH, H<sub>2</sub>O and BeH<sub>2</sub> Calculated at Equilibrium<sup>a</sup>**

	$\Delta E_{\text{CCSD}}$	$\Delta E_{\text{Sym-UCCSD}}^*$	$\Delta E_{\text{CCSD(T)}}$	$\Delta E_{\text{CCSDT-full}}$	$\Delta E_{\text{Sym-UCCSDT}}^*$	FCI
LiH	$1.05 \times 10^{-5}$	$1.06 \times 10^{-5}$	$2.11 \times 10^{-6}$	$2.79 \times 10^{-8}$	$2.16 \times 10^{-8}$	-7.882403410335502
H <sub>2</sub> O	$1.17 \times 10^{-4}$	$1.0 \times 10^{-4}$	$4.91 \times 10^{-5}$	$2.17 \times 10^{-5}$	$2.11 \times 10^{-6}$	-75.01257824109094
BeH <sub>2</sub>	$3.94 \times 10^{-4}$	$3.81 \times 10^{-4}$	$1.84 \times 10^{-4}$	$4.22 \times 10^{-5}$	$6.63 \times 10^{-6}$	-15.595176868923053

<sup>a</sup>The geometry data are taken from the CCCBDB-NIST Database.<sup>54</sup> The UCC-VQE results are referred from Table 2, and those of CCSD, CCSD(T), and CCSDT-full are from Table S5 of the Supplementary Material. The last column represents the FCI energies at STO-3G basis set. The error is the difference between the obtained energy and FCI in (Ha).

between the predicted UCC energy and FCI energy at the STO-3G basis set level. When the molecules are chosen at their equilibrium geometry (see Table 2), the obtained sym-UCCSD error is similar to the one obtained in ref 18, with only a very small difference of  $\approx 10^{-7}$  Ha. The calculated sym-UCCSDT improves the accuracy with respect to sym-UCCSD by about 3 orders of magnitude in LiH and by about 2-order of magnitudes in H<sub>2</sub>O and BeH<sub>2</sub> molecules. This illustrates the capabilities of Triple excitations to recover the correlation energy missed by the sym-UCCSD ansatz at equilibrium. Moreover, we calculate the sym-UCCSD and sym-UCCSDT energies for LiH and BeH<sub>2</sub> at several bond lengths  $R$  ranging between 0.5 and 3.5 Å; see Figure 1. As shown in the figure, in the LiH case, the sym-UCCSD and sym-UCCSDT errors remain below the chemical accuracy for all bond lengths and the difference between sym-UCCSDT and sym-UCCSD errors is again about 3 orders of magnitude smaller. In the BeH<sub>2</sub> case, when  $R$  is 2.0 Å, the sym-UCCSD error starts to get above the chemical accuracy ( $1.6 \times 10^{-3}$  Hartree) and it gets further away as  $R$  increases. Overall, in terms of error, sym-UCCSDT is better than sym-UCCSD by about 1–2 order of magnitudes at all bond lengths. It remains below the chemical accuracy, except when  $R$  is 2.5 Å and beyond, where the error starts to approach the blue line delimiting the chemical accuracy. When  $R$  is equal to 2.75 Å, a discontinuity is observed. In fact, this has been also seen in a previous work (see ref 61) around this bond length in BeH<sub>2</sub> calculated at the STO-3G basis set level. There is one hypothesis which illustrates this anomaly. Indeed, the importance of dynamic correlation starts to increase when the bond length is around 2.7 Å. At this point, according to

Figure 5 in ref 61 the occupation number of the natural orbitals starts to differ from zero or two. Hence many natural orbitals would have significant occupation numbers (i.e., different from zero), so the difference between occupied and virtual orbitals tends to disappear. This probably leads to the inability of our sym-UCCSDT approach to capture some important excitations that might contribute strongly to the dynamical correlation, and thus the sym-UCCSDT errors could increase. In general, this limitation from triple excitations at large bond lengths in BeH<sub>2</sub> can be probably improved by adding higher-order excitations but is consistent with classical coupled cluster behaviors and the limits of single determinant approaches. The data which were used to plot Figure 1 are provided in Tables S4 and S5 from the Supporting Information. In order to compare the classical methods with UCC-VQE simulations, we calculated CCSD, CCSD(T) and CCSDT-full errors for LiH, H<sub>2</sub>O and BeH<sub>2</sub> at equilibrium. The results are shown in Table 3. CCSD and sym-UCCSD errors are very similar. This is also observed in ref 34 where the orbital optimized (OO)-UCCSD method has been tested. The CCSD(T) errors deviate clearly from sym-UCCSDT errors by at least one order of magnitude. sym-UCCSDT also surpasses CCSDT-full (i.e., coupled cluster with a full treatment of singles, doubles and triples) in the three molecules, which is the most remarkable outcome here (see also same behavior in Figure S2(a),(b) of the Supporting Information at some bond lengths in LiH and BeH<sub>2</sub>, respectively). Such behavior has been noticed in ref 37, where it is always CCSDT that has lower quality than UCCSDT, which was calculated analytically.

## CONCLUSION

In conclusion, in this Article, we presented the Trotterized UCCSDT ansatz. We simplified the unitary coupled cluster triple excitation equations by using the spin and point group symmetries. By testing several molecules on QLM simulator, we demonstrated that the efficiency of the symmetric UCCSDT method can be greatly improved. Indeed, reducing the unimportant single, double and triple excitations from the circuit ansatz, one can accelerate the convergence process as well as reduce the circuit depth. Moreover, by performing several numerical simulations, we showed that the symmetric UCCSDT is able to reach a superior accuracy compared to UCCSD (by at least 2 orders of magnitudes). In the future, as quantum simulators and Quantum Processing Units improve and enable researchers to handle more gates, the Trotterized UCCSDT should enable us to perform accurate calculations with large chemical basis sets (i.e., beyond the minimal STO-3G). Overall, the Trotterized UCCSDT can bring interesting results for the general quantum chemistry community since it is shown to be competitive with gold-standard CCSD(T) classical methods.

## ASSOCIATED CONTENT

### Supporting Information

The Supporting Information is available free of charge at <https://pubs.acs.org/doi/10.1021/acs.jpca.3c01753>.

Detailed sketch algorithm that describe the triple excitations within spin and point group symmetries is presented and coded in our openVQE package,<sup>50</sup> convergence study of LiH, data related to the computed total energies for sym-UCCSD and sym-UCCSDT found in Tables S1–S4, comparison of errors between sym-UCCSDT, CCSD(T) and CCSDT-full, and CCSD, CCSD(T) and CCSDT-full total energies (PDF)

## AUTHOR INFORMATION

### Corresponding Authors

**Mohammad Haidar** – Laboratoire de Chimie Théorique, Sorbonne Université, UMR 7616 CNRS, 75005 Paris, France; Sorbonne Université, CNRS, Université Paris Cité, Laboratoire Jacques-Louis Lions (LJLL), 75005 Paris, France; TotalEnergies, 92400 Courbevoie, France; Email: [Mohammadhaidar2016@outlook.com](mailto:Mohammadhaidar2016@outlook.com)

**Jean-Philip Piquemal** – Laboratoire de Chimie Théorique, Sorbonne Université, UMR 7616 CNRS, 75005 Paris, France; [orcid.org/0000-0001-6615-9426](https://orcid.org/0000-0001-6615-9426); Email: [jean-philip.piquemal@sorbonne-universite.fr](mailto:jean-philip.piquemal@sorbonne-universite.fr)

### Authors

**Marko J. Rančić** – TotalEnergies, 92400 Courbevoie, France

**Yvon Maday** – Sorbonne Université, CNRS, Université Paris Cité, Laboratoire Jacques-Louis Lions (LJLL), 75005 Paris, France; Institut Universitaire de France, 75005 Paris, France

Complete contact information is available at: <https://pubs.acs.org/doi/10.1021/acs.jpca.3c01753>

### Notes

The authors declare no competing financial interest.

## ACKNOWLEDGMENTS

M.J.R. acknowledges funding from European Union's Horizon 2020 research and innovation program, more specifically the

(NEIASIQC) project under grant agreement No. 951821. This work has also received funding from the European Research Council (ERC) under the European Union's Horizon 2020 research and innovation program (grant agreement No 810367), project EMC2 (J.P.P., Y.M.). Support from the PEPR EPiQ and HQI programs is acknowledged.

## REFERENCES

- (1) Aspuru-Guzik, A.; Dutoi, A. D.; Love, P. J.; Head-Gordon, M. Simulated quantum computation of molecular energies. *Science* **2005**, *309*, 1704–1707.
- (2) Reiher, M.; Wiebe, N.; Svore, K. M.; Wecker, D.; Troyer, M. Elucidating reaction mechanisms on quantum computers. *Proc. Natl. Acad. Sci. U. S. A.* **2017**, *114*, 7555–7560.
- (3) Bauer, B.; Bravyi, S.; Motta, M.; Chan, G. K.-L. Quantum algorithms for quantum chemistry and quantum materials science. *Chem. Rev.* **2020**, *120*, 12685–12717.
- (4) McArdle, S.; Endo, S.; Aspuru-Guzik, A.; Benjamin, S. C.; Yuan, X. Quantum computational chemistry. *Rev. Mod. Phys.* **2020**, *92*, 015003.
- (5) Bassman, L.; Urbanek, M.; Metcalf, M.; Carter, J.; Kemper, A. F.; de Jong, W. A. Simulating quantum materials with digital quantum computers. *Quantum Science and Technology* **2021**, *6*, 043002.
- (6) Gan, Z.; Grant, D. J.; Harrison, R. J.; Dixon, D. A. The lowest energy states of the group-III A–group-VA heteronuclear diatomics: BN, BP, AlN, and AlP from full configuration interaction calculations. *J. Chem. Phys.* **2006**, *125*, 124311.
- (7) Lehtola, S.; Tubman, N. M.; Whaley, K. B.; Head-Gordon, M. Cluster decomposition of full configuration interaction wave functions: A tool for chemical interpretation of systems with strong correlation. *J. Chem. Phys.* **2017**, *147*, 154105.
- (8) Vogiatzis, K. D.; Ma, D.; Olsen, J.; Gagliardi, L.; De Jong, W. A. Pushing configuration-interaction to the limit: Towards massively parallel MCSCF calculations. *J. Chem. Phys.* **2017**, *147*, 184111.
- (9) Peruzzo, A.; McClean, J.; Shadbolt, P.; Yung, M.-H.; Zhou, X.-Q.; Love, P. J.; Aspuru-Guzik, A.; O'Brien, J. L. A variational eigenvalue solver on a photonic quantum processor. *Nat. Commun.* **2014**, *5*, 4213.
- (10) McClean, J. R.; Romero, J.; Babbush, R.; Aspuru-Guzik, A. The theory of variational hybrid quantum-classical algorithms. *New J. Phys.* **2016**, *18*, 023023.
- (11) Cerezo, M.; Arrasmith, A.; Babbush, R.; Benjamin, S. C.; Endo, S.; Fujii, K.; McClean, J. R.; Mitarai, K.; Yuan, X.; Cincio, L.; et al. Variational quantum algorithms. *Nature Reviews Physics* **2021**, *3*, 625–644.
- (12) Li, W.; Huang, Z.; Cao, C.; Huang, Y.; Shuai, Z.; Sun, X.; Sun, J.; Yuan, X.; Lv, D. Toward practical quantum embedding simulation of realistic chemical systems on near-term quantum computers. *Chemical science* **2022**, *13*, 8953–8962.
- (13) O'Malley, P. J.; Babbush, R.; Kivlichan, I. D.; Romero, J.; McClean, J. R.; Barends, R.; Kelly, J.; Roushan, P.; Tranter, A.; Ding, N.; et al. Scalable quantum simulation of molecular energies. *Physical Review X* **2016**, *6*, 031007.
- (14) Bharti, K.; Cervera-Lierta, A.; Kyaw, T. H.; Haug, T.; Alperin-Lea, S.; Anand, A.; Degroote, M.; Heimonen, H.; Kottmann, J. S.; Menke, T.; et al. Noisy intermediate-scale quantum algorithms. *Rev. Mod. Phys.* **2022**, *94*, 015004.
- (15) Kühn, M.; Zanker, S.; Deglmann, P.; Marthaler, M.; Weiß, H. Accuracy and resource estimations for quantum chemistry on a near-term quantum computer. *J. Chem. Theory Comput.* **2019**, *15*, 4764–4780.
- (16) Lolur, P.; Rahm, M.; Skogh, M.; García-Álvarez, L.; Wendin, G. Benchmarking the variational quantum eigensolver through simulation of the ground state energy of prebiotic molecules on high-performance computers. *AIP Conference Proceedings*; AIP, 2021; p 030005.
- (17) Yeter-Aydeniz, K.; Gard, B. T.; Jakowski, J.; Majumder, S.; Barron, G. S.; Siopsis, G.; Humble, T. S.; Pooser, R. C. Benchmarking

quantum chemistry computations with variational, imaginary time evolution, and Krylov space solver algorithms. *Advanced Quantum Technologies* **2021**, *4*, 2100012.

(18) Cao, C.; Hu, J.; Zhang, W.; Xu, X.; Chen, D.; Yu, F.; Li, J.; Hu, H.-S.; Lv, D.; Yung, M.-H. Progress toward larger molecular simulation on a quantum computer: Simulating a system with up to 28 qubits accelerated by point-group symmetry. *Phys. Rev. A* **2022**, *105*, 062452.

(19) Arute, F.; Arya, K.; Babbush, R.; Bacon, D.; Bardin, J. C.; Barends, R.; Boixo, S.; Broughton, M.; Buckley, B. B.; et al. Hartree-Fock on a superconducting qubit quantum computer. *Science* **2020**, *369*, 1084–1089.

(20) Kandala, A.; Mezzacapo, A.; Temme, K.; Takita, M.; Brink, M.; Chow, J. M.; Gambetta, J. M. Hardware-efficient variational quantum eigensolver for small molecules and quantum magnets. *Nature* **2017**, *549*, 242–246.

(21) Hempel, C.; Maier, C.; Romero, J.; McClean, J.; Monz, T.; Shen, H.; Jurcevic, P.; Lanyon, B. P.; Love, P.; Babbush, R.; et al. Quantum chemistry calculations on a trapped-ion quantum simulator. *Physical Review X* **2018**, *8*, 031022.

(22) Tazhigulov, R. N.; Sun, S.-N.; Haghshenas, R.; Zhai, H.; Tan, A. T.; Rubin, N. C.; Babbush, R.; Minnich, A. J.; Chan, G. K.-L. Simulating Models of Challenging Correlated Molecules and Materials on the Sycamore Quantum Processor. *PRX Quantum* **2022**, *3*, 040318.

(23) Crawford, T. D.; Schaefer, H. F., III An introduction to coupled cluster theory for computational chemists. *Reviews in computational chemistry* **2007**, *14*, 33–136.

(24) Bartlett, R. J.; Musial, M. Coupled-cluster theory in quantum chemistry. *Rev. Mod. Phys.* **2007**, *79*, 291.

(25) Romero, J.; Babbush, R.; McClean, J. R.; Hempel, C.; Love, P. J.; Aspuru-Guzik, A. Strategies for quantum computing molecular energies using the unitary coupled cluster ansatz. *Quantum Science and Technology* **2019**, *4*, 014008.

(26) Anand, A.; Schleich, P.; Alperin-Lea, S.; Jensen, P. W.; Sim, S.; Diaz-Tinoco, M.; Kottmann, J. S.; Degroote, M.; Izmaylov, A. F.; Aspuru-Guzik, A. A quantum computing view on unitary coupled cluster theory. *Chem. Soc. Rev.* **2022**, *51*, 1659–1684.

(27) Hatano, N.; Suzuki, M. *Quantum annealing and other optimization methods*; Springer, 2005; pp 37–68.

(28) Sokolov, I. O.; Barkoutsos, P. K.; Ollitrault, P. J.; Greenberg, D.; Rice, J.; Pistoia, M.; Tavernelli, I. Quantum orbital-optimized unitary coupled cluster methods in the strongly correlated regime: Can quantum algorithms outperform their classical equivalents? *J. Chem. Phys.* **2020**, *152*, 124107.

(29) Xia, R.; Kais, S. Qubit coupled cluster singles and doubles variational quantum eigensolver ansatz for electronic structure calculations. *Quantum Science and Technology* **2021**, *6*, 015001.

(30) Grimsley, H. R.; Claudino, D.; Economou, S. E.; Barnes, E.; Mayhall, N. J. Is the trotterized uccsd ansatz chemically well-defined? *J. Chem. Theory Comput.* **2020**, *16*, 1–6.

(31) Yung, M.-H.; Casanova, J.; Mezzacapo, A.; McClean, J.; Lamata, L.; Aspuru-Guzik, A.; Solano, E. From transistor to trapped-ion computers for quantum chemistry. *Sci. Rep.* **2014**, *4*, 3589.

(32) Shen, Y.; Zhang, X.; Zhang, S.; Zhang, J.-N.; Yung, M.-H.; Kim, K. Quantum implementation of the unitary coupled cluster for simulating molecular electronic structure. *Phys. Rev. A* **2017**, *95*, 020501.

(33) O'Brien, T. E.; Anselmetti, G.; Gkritsis, F.; Elfving, V.; Polla, S.; Huggins, W. J.; Oumarou, O.; Kechedzhi, K.; Abanin, D.; Acharya, R. Purification-based quantum error mitigation of pair-correlated electron simulations. *arXiv preprint arXiv:2210.10799* **2022**, DOI: 10.48550/arXiv.2210.10799.

(34) Mizukami, W.; Mitarai, K.; Nakagawa, Y. O.; Yamamoto, T.; Yan, T.; Ohnishi, Y.-y. Orbital optimized unitary coupled cluster theory for quantum computer. *Physical Review Research* **2020**, *2*, 033421.

(35) Sennane, W.; Piquemal, J.-P.; Rančić, M. J. Calculating the ground-state energy of benzene under spatial deformations with noisy quantum computing. *Phys. Rev. A* **2023**, *107*, 012416.

(36) Lee, J.; Huggins, W. J.; Head-Gordon, M.; Whaley, K. B. Generalized unitary coupled cluster wave functions for quantum computation. *J. Chem. Theory Comput.* **2019**, *15*, 311–324.

(37) Köhn, A.; Olsen, J. Capabilities and limits of the unitary coupled-cluster approach with generalized two-body cluster operators. *J. Chem. Phys.* **2022**, *157*, 124110.

(38) Grimsley, H. R.; Economou, S. E.; Barnes, E.; Mayhall, N. J. An adaptive variational algorithm for exact molecular simulations on a quantum computer. *Nat. Commun.* **2019**, *10*, 3007.

(39) Fedorov, D. A.; Alexeev, Y.; Gray, S. K.; Otten, M. Unitary Selective Coupled-Cluster Method. *Quantum* **2022**, *6*, 703.

(40) Smart, S. E.; Boyn, J.-N.; Mazziotti, D. A. Resolving correlated states of benzene with an error-mitigated contracted quantum eigensolver. *Phys. Rev. A* **2022**, *105*, 022405.

(41) Smart, S. E.; Mazziotti, D. A. Quantum solver of contracted eigenvalue equations for scalable molecular simulations on quantum computing devices. *Phys. Rev. Lett.* **2021**, *126*, 070504.

(42) Raghavachari, K. Historical perspective on: A fifth-order perturbation comparison of electron correlation theories [Volume 157, Issue 6, 26 May 1989, Pages 479–483]. *Chem. Phys. Lett.* **2013**, *589*, 35–36.

(43) Ramabhadran, R. O.; Raghavachari, K. Extrapolation to the gold-standard in quantum chemistry: computationally efficient and accurate CCSD (T) energies for large molecules using an automated thermochemical hierarchy. *J. Chem. Theory Comput.* **2013**, *9*, 3986–3994.

(44) Dresselhaus, M. S.; Dresselhaus, G.; Jorio, A. *Group theory: application to the physics of condensed matter*; Springer Science & Business Media, 2007.

(45) Tinkham, M. *Group Theory and Quantum Mechanics*; McGraw-Hill: New York, 1964.

(46) Atkins, P. W.; Child, M. S.; Phillips, C. S. G. *Tables for group theory*; Oxford University Press: Oxford, 1970; Vol. 6.

(47) Fradkin, E. Jordan-Wigner transformation for quantum-spin systems in two dimensions and fractional statistics. *Physical review letters* **1989**, *63*, 322.

(48) ATOS, myqlm-fermion. Repository: <https://github.com/myQLM/myqlm-fermion>. Documentation: <https://myqlm.github.io/qat-fermion.html>.

(49) Haidar, M.; Rančić, M. J.; Ayral, T.; Maday, Y.; Piquemal, J.-P. Open source variational quantum eigensolver extension of the quantum learning machine for quantum chemistry. *WIREs Computational Molecular Science* **2023**, e1664.

(50) Haidar, M.; Rančić, M. J.; Maday, Y.; Piquemal, J.-P. OpenVQE package. Repository: <https://github.com/OpenVQE/OpenVQE.git>. Documentation: <https://openvqe.github.io/OpenVQE/>.

(51) Sun, Q.; Berkelbach, T. C.; Blunt, N. S.; Booth, G. H.; Guo, S.; Li, Z.; Liu, J.; McClain, J. D.; Sayfutyrova, E. R.; Sharma, S.; et al. PySCF: the Python-based simulations of chemistry framework. *Wiley Interdisciplinary Reviews: Computational Molecular Science* **2018**, *8*, No. e1340.

(52) Virtanen, P.; Gommers, R.; Oliphant, T. E.; Haberland, M.; Reddy, T.; Cournapeau, D.; Burovski, E.; Peterson, P.; Weckesser, W.; Bright, J.; et al. SciPy 1.0: fundamental algorithms for scientific computing in Python. *Nat. Methods* **2020**, *17*, 261–272.

(53) Smith, D. G.; Burns, L. A.; Simmonett, A. C.; Parrish, R. M.; Schieber, M. C.; Galvelis, R.; Kraus, P.; Kruse, H.; Di Remigio, R.; Alenaizan, A.; et al. PSI4 1.4: Open-source software for high-throughput quantum chemistry. *J. Chem. Phys.* **2020**, *152*, 184108.

(54) Johnson, R. *Computational Chemistry Comparison and Benchmark Database*; NIST, 2018; <http://cccbdb.nist.gov/>, DOI: 10.18434/T47C7Z.

(55) Hehre, W.; Ditchfield, R.; Stewart, R.; Pople, J. self-consistent molecular orbital methods. iv. use of Gaussian expansions of Slater-

type orbitals. Extension to second-row molecules. *J. Chem. Phys.* **1970**, *52*, 2769–2773.

(56) Barkoutsos, P. K.; Gonthier, J. F.; Sokolov, I.; Moll, N.; Salis, G.; Fuhrer, A.; Ganzhorn, M.; Egger, D. J.; Troyer, M.; Mezzacapo, A.; et al. Quantum algorithms for electronic structure calculations: Particle-hole Hamiltonian and optimized wave-function expansions. *Phys. Rev. A* **2018**, *98*, 022322.

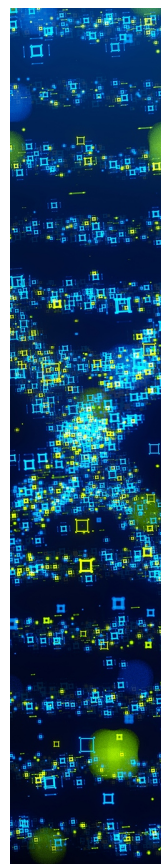
(57) Evangelista, F. A.; Chan, G. K.-L.; Scuseria, G. E. Exact parameterization of fermionic wave functions via unitary coupled cluster theory. *J. Chem. Phys.* **2019**, *151*, 244112.

(58) Izmaylov, A. F.; Diaz-Tinoco, M.; Lang, R. A. On the order problem in construction of unitary operators for the variational quantum eigensolver. *Phys. Chem. Chem. Phys.* **2020**, *22*, 12980–12986.

(59) Whitfield, J. D.; Biamonte, J.; Aspuru-Guzik, A. Simulation of electronic structure Hamiltonians using quantum computers. *Mol. Phys.* **2011**, *109*, 735–750.

(60) Magoulas, I.; Evangelista, F. A. CNOT-Efficient Circuits for Arbitrary Rank Many-Body Fermionic and Qubit Excitations. *J. Chem. Theory Comput.* **2023**, *19* (3), 822–836.

(61) Van Raemdonck, M.; Alcoba, D. R.; Poelmans, W.; De Baerdemacker, S.; Torre, A.; Lain, L.; Massaccesi, G. E.; Van Neck, D.; Bultinck, P. Polynomial scaling approximations and dynamic correlation corrections to doubly occupied configuration interaction wave functions. *J. Chem. Phys.* **2015**, *143*, 104106.



CAS BIOFINDER DISCOVERY PLATFORM™

## STOP DIGGING THROUGH DATA —START MAKING DISCOVERIES

CAS BioFinder helps you find the  
right biological insights in seconds

Start your search

